Silicon (2015) 7:297–302
DOI 10.1007/s12633-014-9275-2

ORIGINAL PAPER

# Study of the Electron Lifetime in Crystalline and Multicrystalline Si Solar Cells

**A. A. El-Amin**

Received: 10 August 2014 / Accepted: 18 December 2014 / Published online: 14 February 2015


**Abstract** Crystalline (including multicrystalline) silicon based devices dominate the present solar cell industry due to their durability, relatively low cost, and the vast silicon knowledge base developed by the microelectronics industry. Multicrystalline silicon is becoming the dominating substrate material of the photovoltaic cells. This is obviously due to the significant cost savings compared with the single crystalline silicon wafers. Consequently, the conversion efficiency of the mc-Si solar cell is suffering because of the low cost requirement of the starting materials. One contributor to the lower performance of the mc-Si cells is the grain boundaries which reduce the charge carrier collection properties. Thus, reducing solar cell fabricate is an attractive way to reduce material costs. However, the model calculations in the presented paper show that the rear surface recombination velocity (S) in multicrystalline silicon cell is greater than (mc-Si) cell and the efficiency of mc-Si cell is lower than the efficiency of a crystalline cell.

**Keywords** Crystalline & multicrystalline Si · Electron lifetime · Model calculation

A. A. El-Amin (✉)
Physics Department, Faculty of Science, Yanbu,
Taibah University, Kingdom of Saudi Arabia,
Madina, Saudi Arabia
e-mail: aaelamin2000@yahoo.com

A. A. El-Amin
Physics Department, Faculty of Science, Aswan University,
81528 Aswan, Egypt

## 1 Introduction

About 40–50 % of the cost of a photovoltaic module is associated with silicon material growth and wafering [1–4]. Nevertheless, in order to lower the cost of silicon solar cells, reduction in cell thickness is being actively investigated [1, 5]. One challenge facing manufacturing thin solar cells is rear surface passivation, because implementation of the standard aluminum back surface field (Al BSF) can cause thin wafers ($\leq$ 150 µm) to warp, resulting in unacceptable yield [6]. Accordingly, dielectric rear passivation is being pursued [7]. While dielectric passivation has been used to achieve a surface recombination velocity (S) as low as 4 cm/s on 1.5 Ω-cm crystalline substrates [8], it is unclear whether the same dielectric can passivate the multicrystalline silicon surface as effectively as the crystalline surface. Defects, like grain boundaries and dislocations at the multicrystalline silicon/dielectric interface may affect passivation. Since S may be different on identically processed crystalline and multicrystalline silicon, its values on crystalline silicon should not be used when modeling multicrystalline devices.

If a small S is assumed, modeling indicates that reducing cell thickness (W) from 300 µm to 100 µm improves efficiency [5], whereas the opposite result is true if S is high. This is demonstrated by the simulation results of Fig. 1 for a bulk lifetime ($\tau_b$) of 20 µs, approximately 1000 cm/s is the S value below which thinner cells are superior and above which thicker cells are superior. It has been experimentally verified that efficiency improves as BSF cells are thinned, whereas efficiency decreases when cells with poorly passivated rear surfaces are thinned [9]. Thus when considering thickness reductions of multicrystalline devices, in order to

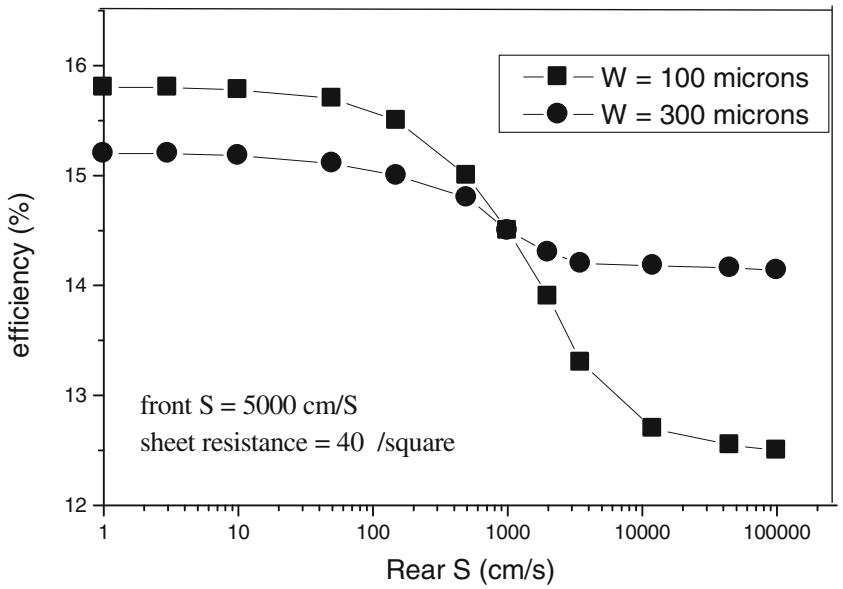


**Fig. 1** Simulation demonstrating that thinner cells perform better for S < 1000 cm/s, whereas thicker cells perform better for S > 1000 cm/s

reduce material costs, one must know S well enough to determine whether efficiency will improve or decline with decreasing thickness.

This paper presents the results of measurements of spatially averaged S on dielectric-passivated string ribbon using quasi-steady-state photoconductance. In order to determine S, the contributions of both S and $\tau_b$ to the effective lifetime ($\tau_{eff}$) must be separated. Every known method for suppressing S to determine $\tau_b$ has its drawbacks, as described in [10]. Additionally, it is recently shown [11] that while an iodine/methanol solution [12] reliably passivates the crystalline silicon surface more effectively than the dielectrics under investigation, the string ribbon silicon surface is often less effectively passivated by the iodine/methanol solution than the dielectrics. So, the iodine/methanol solution cannot be used to suppress S for the separation of surface and bulk recombination in materials like string ribbon silicon. Given the failure of the iodine/methanol solution to determine $\tau_b$ accurately enough to calculate S on string ribbon silicon, the method described in [12] was applied and two illuminating spectra were used to measure $\tau_{eff}$. Assuming that ±10 % uncertainty in $\tau_{eff}$ measured with each spectrum, it is found that a region in the S-$\tau_b$ plane consistent with each measurement. The intersection of the regions given by the two $\tau_{eff}$ measurements provides a range of S and $\tau_b$ values consistent with the two measurements. The region bounded by the solid lines is consistent with $\tau_{eff}$ measurements using 500 nm illuminations, and the region bounded by the broken lines is consistent with $\tau_{eff}$ measurements using 1000 nm illumination; the intersection thus gives the region in the S-$\tau_b$ plane consistent with both measurements. In this case, it was found that 390 cm/s < S < 4500 cm/s. Using this method, determination of S on dielectric-passivated crystalline and multicrystalline silicon, was proceeded.

## 2 Method

### 2.1 Experimental Details

Two kinds of silicon materials were selected in the present study, single crystal of 0.7 Ω.cm, and a multicrystalline of 2.9 Ω.cm resistivity with thickness 270 µm., and the wafers were cleaned in standard chemical solutions. Subsequently, a wafer of each type was processed in one of the following three ways, to stack passivation, 100 Å thermal oxide grown at 925 °C in a tube furnace followed by deposition at 300 °C of 850 Å high-frequency. All wafers received a 20 minute forming gas: $N_2$ + $H_2$, (FGH) anneal at 400 °C. $\tau_{eff}$ was measured under both 500 nm and 1000 nm illumination. This illumination was achieved by using monochromatic optical filters with bandwidths of 71 nm and 16 nm, respectively. The lifetime measurements were analyzed to extract S ranges according to the method introduced in [12], elaborated in [13]. Since the inductive coil used to measure photoconductance is larger than a single grain, this technique gives a spatially averaged S. For the string ribbon wafers, an $\tau_{eff}$ error of ±5 % was also used for comparison. Each wafer had a different range of injection levels accessible to measurement, due to nonrecombinative trapping [14] and the optical filters. Thus, it was not possible to measure $\tau_{eff}$ at the same injection level on each wafer. The injection levels at which $\tau_{eff}$ was measured range from $5\times10^{13}-2\times10^{15}$ $cm^{-3}$, with similarity as possible for injection levels chosen for all wafers of a given material.

### 2.2 Theory

Recently, a new class of photo metal cells based on semicondctors (solar cell) has promoted intense research due to

the prospects of cheap and efficient conversion of visible light into electricity and of new applications such as transparent solar cells [15]. It is widely agreed that the electron-transfer kinetics play a major role in determining the energy conversion efficiency of dye-sensitized solar cells [16, 17]. Herein, a new powerful tool was developed to study the electron lifetime in solar cells as a function of the photovoltage ($V_{oc}$); the open-circuit voltage (OCV) technique. This technique has certain advantages over frequency or steady-state-based methods: a) it provides a continuous reading of the lifetime as a function of $V_{oc}$ at high-voltage resolution, b) it is experimentally much simpler, and c) the data treatment is outstandingly simple (basically, it consists of two derivatives) for obtaining the main quantities that provide information on the recombination mechanisms. In order to treat such data and their obtained analyses a new theoretical framework that derives the electron lifetime from a general recombination rate, (U(n)), was presented. It incorporates the possible complex-recombination mechanisms in dye solar cells, such as a higher reaction order electron transfer mediated by trapping and de-trapping. These mechanisms will be conveniently represented by an effective recombination order ($\beta$) that governs the change of the lifetime over a broad variation of internal conditions in the solar cell. A procedure to extract the fundamental information on the electron lifetime from the measured OCV curves will provide also. The equivalence, in broad terms, with the lifetime, measured by intensity-modulated photovoltage spectroscopy (IMVS), a well as, the unique observations revealed by the high voltage resolution will be shown. When the cell is illuminated at open circuit, the free electron density in the semiconductor nanostructure (n) is affected by two main processes. 1) Electron photogeneration, which is achieved by electron injection from the photogeneration molecules attached to the semiconductor nanoparticle surface into the semiconductor conduction band (cb), that is, photogeneration of the dye molecules. This photogeneration process can be maintained at a stationary rate, since the reduced electrolyte species (electron donors) are able to regenerate the oxidized dye molecules. 2) Recombination of the photogenerated electrons, which is thought to be predominant in comparison with electron capture. Therefore, n increases by photogeneration at a rate $G = a_{abs}\ I_0$, where $I_0$, the incident light intensity, $a_{abs}$, is the absorption coefficient of dye molecules and homogeneous photoinjection is assumed, and decreases by recombination at a rate U(n) that depends on the electron density in the electrode. The overall balance can be expressed by the kinetic Eq. 1.

$$dn\backslash dt = -U(n) + a_{abs}I_0 \tag{1}$$

Under constant illumination, the solar cell reaches a photostationary situation in which the free electron density satisfies $U(n) + a_{abs}I_0$. Under these conditions, $V_{oc}$ corresponds to the increase of the quasi-Fermi level of the semiconductor ($E_{Fn}$) with respect to the dark value ($E_{F0}$), which equals the electron energy ($E_{F0} = E_{redox}$). Therefore, it can be written as Eq. 2 [13]

$$V_{oc} = E_{Fn}\text{-}E_{F0}/\mathbf{e} = [k_BT/e]\ \ln\ [n/n_0] \tag{2}$$

Here, $k_BT$ is the thermal energy, e is the positive elementary charge, and $n_0$ is the concentration in the dark. Clearly, the recombination rate has a major impact on the open-circuit voltage obtained at any light intensity. Information on the properties of the recombination process can be obtained from the correlation $V_{oc}(I_0)$ in the steady state. A much more sensitive method is to determine the characteristic time of recovery when the system is displaced from a steady state at open circuit, that is, the electron lifetime ($\tau_n$). In the solar-cell area, the dominant dynamic technique of this kind is IMVS, which measures the photovoltage in response to a small periodic modulation of the light intensity over a background steady state [15, 16]. Another way to probe the kinetics of recombination is to monitor the transient of $V_{oc}$ during the relaxation from the illuminated quasiequilibrium state to the dark equilibrium. Although this method is fairly obvious, as far as it known, it has not been fully developed for the study of solar cells. A possible reason for this is the huge variation of the photophysical magnitudes in this system when the steady state is varied. Indeed, the results of IMVS showed that the electron lifetime changes exponentially over orders of magnitude when the steady state varies from $V_{oc} = 0$ V to the upper limit, which is $\approx 0.8$ V [10, 11]. Therefore, large perturbation techniques involving vast changes of the parameters will, in principle, be much more difficult to interpret than those techniques that function by a small perturbation over a steady state, such as IMVS. However, in the following it is showed that it is indeed possible to obtain the (variable) electron lifetime from large amplitude OCV technique. This is facilitated by the fact that in the OCV the system is kept at open circuit during the transient, and because the internal gradients of carriers are usually low, the measurements of $V_{oc}(t)$ very nearly records a succession of steady states. The starting point for the $V_{oc}$ decaymeasurement is the non equilibrium steady state of a cell illuminated at constant intensity $I_0$. The illumination is interrupted, and $V_{oc}(t)$ is recorded, while the cell is kept at open circuit. During the decay, n evolves from the initial steady state value to the dark equilibrium ($V_{oc} = 0$) with concentration $n_0$. The final region of decay at $V_{oc} \approx 50$ mV or less, which is poorly resolved in the current setup, will generally be neglected, hence it was assumed that $n << n_0$. According to Eq. 1, the transient was described by Eq. 3:

$$dn\backslash dt = -U\ (n) \tag{3}$$

Intuitively, the electron lifetime can be defined as Eq. 4:

$$\tau^{-1} = -(dn\backslash ndt) \tag{4}$$

Hence, Eq. 5 could obtain as follows:

$$\tau_n = n / U(n) \tag{5}$$

This definition is exact only for a linear system with $U = k_r n$ ($k_r$ = rate constant for recombination) [17]. The more general and rigorous concept of the lifetime was discussed below, and it was shown that Eq. 5 is generally justified for the decay in nonlinear solar cells. Using Eqs. 2 and 5, it can derive the lifetime from $V_{oc}(t)$ by Eq. 6:

$$\tau_n = K_B T/e\,(dV_\infty/dt)^{-1} \tag{6}$$

Therefore, $\tau_n(V_{oc})$ is given by the reciprocal of the derivative of the decay curve normalized by the thermal voltage.

It has been suggested that the recombination reaction in dye solar cells (mediated by the electron acceptor $I_2$) is nonlinear, and of second order with respect to electron concentration, [19–21] in which case $U \propto n^2$. Let us consider the nonlinear recombination model, Eq. 7:

$$U = K_r n^\beta \tag{7}$$

Where $\beta$ is a constant. By Eq. 5, the lifetime takes the form of Eq. 8:

$$\tau_n = 1/K_r n^{\beta-1} \tag{8}$$

It is noticed, Eq. 8, that the effective recombination order can be obtained as Eq. 9:

$$\beta = 1 + \left[d\ln\tau_n^{-1}/d\ln n\right] \tag{9}$$

In order to characterize in detail the variation of the lifetime, Eq. 9 was taken as a general definition of the $\beta$ parameter without assuming its constancy. When lets as $\beta$ an arbitrary function of the Fermi level, it was able to express any recombination mechanism in terms of this parameter (not only the second-order reaction, $\beta = 2$, which was taken as an intuitive starting point), by writing the recombination rate as in Eq. 7. The $\beta$ parameter is a convenient description of the lifetime-dependence on the Fermi level in dye solar cells because experimentally Eq. 9 is found to be nearly constant. But the parameter $\beta$ takes physical content when a specific kinetic model for recombination is formulated, so that the model implications can be compared with the measurements; this will be illustrated below with a model including trapping effects.

By substituting Eq. 2 instead Eq. 9, the expression, Eq. 10 was obtained:

$$\beta = 1 + (K_B T/e)(d\ln\tau_n^{-1}/d\,V_\infty) \tag{10}$$

The current transport processes through the cells have been studied the diffusion theory of the conductivity for crystals [15, 16], and the theory of the current transport

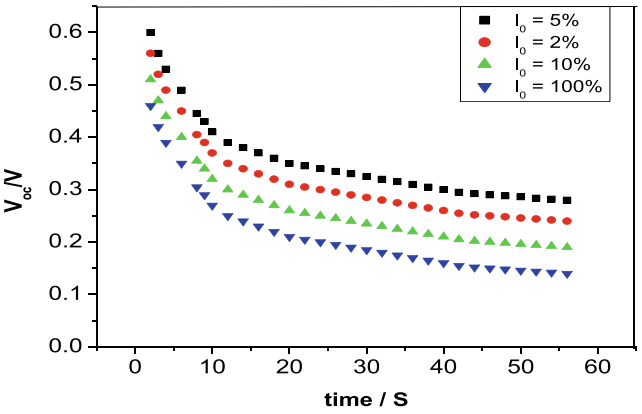


**Fig. 2** Experimental $V_{oc}$ decay results of a single crystalline solar cell starting at four different initial steady states, as indicated by the relative incident light intensities in the solar cell

approximation [17]. Within the first one, the following current-voltage dependence take place for $U << q/(\alpha KT)$:

$$J = J_0(1 - 4a_2U_2)\exp(q/2KT\alpha)(U - aU_2) \tag{11}$$

$$J_0 = (\mu KTN_s/4L_2)\exp[-\Phi_0/KT] \tag{12}$$

Here $U = \alpha V$ is the net voltage, q is the electronic charge, $\varepsilon$ is the dielectric constant.

## 3 Results and Discussions

The results of the measurements and the application of the procedures of analysis outlined above are presented in Figs. 2 and 3. The data shown in these figures reveled four OCVD decay curves starting at different initial steady states at progressively lower light intensities. For a linear system with a unique $\tau_n$, the $V_{oc}(t)$ characteristics would decay linearly with time. In fact, the results show the obtained lifetime

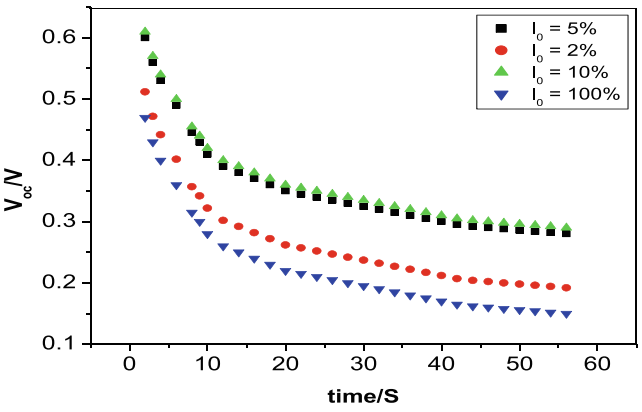


**Fig. 3** Experimental $V_{oc}$ decay results of a multicrystalline solar cell starting at four different initial steady states, as indicated by the relative incident light intensities in the solar cell

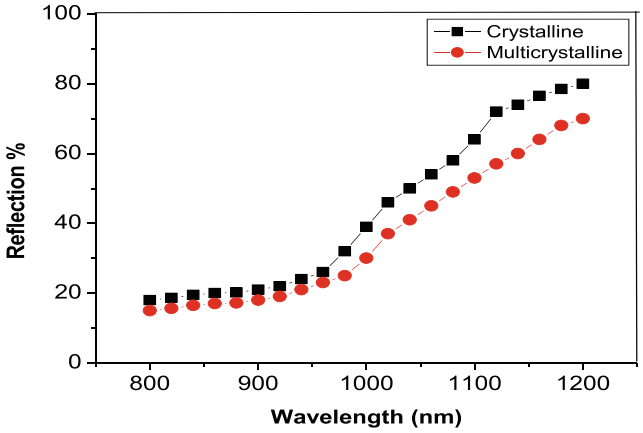


**Fig. 4** Measured hemispherical reflectance of solar cells with a crystalline wafer and mc-Si

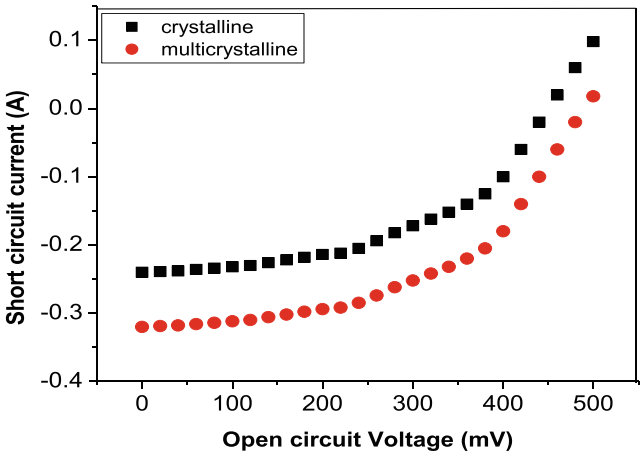


**Fig. 5** I-V characteristics for crystalline and multicrystalline Si solar cells

values using Eq. 6. The lifetime dependence on $V_{oc}$ is exponential in broad terms, spanning three decades from 20 ms to 20 s when $V_{oc}$ decreases starting at $\approx 0.6$ V.

An important loss mechanism for thin silicon solar cells are optical losses. Due to the relatively low absorption coefficient of silicon, a very good light trapping is needed if the solar cell thickness is reduced. For multicrystalline silicon wafers the standard light trapping schemes like random pyramids are not homogeneous due to the different crystallographic orientations of the grains. A second problem, occurs if surface texturing with random pyramids is applied to thin silicon wafers, is a severe reduction in mechanical stability.

The planar mc-Si wafers cell process, with a single-layer antireflection coating was used in the present study. The hemispherical reflectance of two solar cells with identical grain structure is shown in Fig. 4. Only the wavelength range between 800 nm and 1150 nm is plotted since it is the range where a difference is expected, due to variation in internal reflectance. The reflectance for the 300 µm and 200 µm thick solar cells is nearly identical for each type of rear surface structure. So, the loss in $J_{sc}$ due to reduced absorption can be neglected for the 200 µm thick devices. This was also demonstrated by other groups on large area screen printed mc-Si solar cells [21].

Another point is the output parameters of the two cells. Due to compare the best data of the wafers, as shown in Table 1, and Fig. 5 fill factors of 75.3–66.4 % leading to cell efficiencies of 14 % about crystalline, and 11.8 about mc-Si were obtained.

The results of two cell specimens are given in Fig. 5. It can be noted that, the advantage of using the crystalline cell, and the short circuit current ($I_{sc}$) of the cell give the value of 31.8 mA, and mc-Si gives 22.5 mA, in addition to enhancement in the open circuit voltage, Fill Factor, and efficiency for the specimen.

Table 1, illuminated I-V-parameters of two solar cells using the standard process shown in Fig. 5.

**Table 1** Illuminated I-V-parameters of two solar cells

| Cell parameters | $I_{sc}$[mA] | $V_{oc}$[mV] | FF [%] | η[%] |
|---|---|---|---|---|
| crystalline | 31.8 | 520 | 75.3 | 14 |
| mc-Si | 22.5 | 350 | 66.4 | 11.8 |

## 4 Conclusions

The present study had shown that the analyses of the decay of photovoltage at open-circuit conditions in dye solar cells constitute a very simple procedure for obtaining the relevant information on the electron lifetime $\tau_n$. It also shown the parameter $\beta$ (effective recombination order) that governs the change of the lifetime. It was found that the lifetime dependence on $V_{oc}$ is exponential in broad terms, spanning three decades from 20 ms to 20 s. Thinning wafers to reduce cost may have the undesired consequence of reducing efficiency unless rear S is sufficiently low. The cell silicon process had been applied to thin multicrystalline silicon wafers and crystalline. Cell efficiencies up to 14 % were achieved about crystalline and 11.8 % for multicrystalline.

**Acknowledgments** The financial support of the Scientific Research Deanship of Taibah University (grant number 6278) is acknowledged.

## References

1. Axelevitch A, Palankovski V, Selberherr S, Golan G (2014) Investigation of novel silicon PV cells of a lateral type. In: Silicon, pp 1–9

2. Slaoui A, Siffert P (2004) Polycrystalline silicon films for electronic devices. In: Silicon, pp 49–72
3. Muller JC, Siffert P (2004) Silicon for photovoltaics. In: Silicon, pp 73–92
4. Dornich K, Schüler N, Berger B, Niklas JR (2013) Fast, high resolution, inline contactless electrical semiconductor characterization for photovoltaic applications by microwave detected photoconductivity. Mater Sci Eng B
5. Rohatgi A, Ebong A, Yelundur V, Ristow A (1999) Rapid thermal processing of next generation silicon solar cells. In: 10th international workshop on the physics of semiconductor devices, pp 14–18
6. Schneider A et al (2001) Al BSF for thin screenprinted multicrystalline Si solar cells. In: 17th EU-PVSEC
7. Aberle A, Warta W, Knobloch J, Voss B (1990) Surface passivation of high efficiency silicon solar cells, In: 21st IEEE PVSC, pp 233–238
8. Lauinger T, Schmidt J, Aberle A, Hezel R (1996) Recond low surface recombination velocities on 1 Ω-cm psilicon using remote plasma silicon nitride passivation. Appl Phys Lett 68:1232–1234
9. Koval T, Wohlegemuth J, Kinsey B (1996) Dependence of cell performance on wafer thickness for BSF and non-BSF cells. In: 25th IEEE PVSC, pp 505–507
10. Schulenburg H, Tributsch H (2000) Electropassivation of silicon and bulk lifetime determination with dry polymer contact. J Phys D 33:851–858
11. Brody J, Rohatgi A (2002) Sensitivity analysis of twospectrum separation of surface and bulk components of minority carrier lifetime. Solid State Electron 46:859–866
12. M'Saad H, Michel J, Lappe JJ, Kimerling LC (1994) Electronic passivation of silicon surfaces by halogens. J Elec Mat 23:487–491
13. Bail M, Brendel R (2000) Separation of bulk and surface recombination by steady state photoconductance measurements." In: 16th European PV conference
14. Macdonald D, Sinton RA, Cuevas A (2001) On the use of a bias-light correction for trapping effects in photoconductance- based lifetime measurements of silicon. J Appl Phys 89:2772–2778
15. O'Regan B, Grätzel M (1991) Nature 353:737
16. Bisquert J, Zaban A, Salvador P (2002) J Phys Chem B 106:8774
17. Montanari I, Nelson J, Durrant JR (2002) J Phys Chem B 106:12203
18. Schlichthörl G, Huang SY, Sprague J, Frank AJ (1997) J Phys Chem B 101:8141
19. Fisher AC, Peter LM, Ponomarev EA, Walker AB, Wijayantha KGU (2000) J Phys Chem B 104:949
20. Södergren S, Hagfeldt A, Olsson J, Lindquist SE (1994) J Phys Chem 98:5552
21. Tools CJJ, Burgers AR, Manshanden P, Weeber AW, von Straaten BHM (2002) Influence of wafer thickness on the performance of multicrystalline Si solar cells: an Experimental Study. Prog Photovolt Res Appl 10:279–291